Letter Vol. 2, No. 4 / April 2015 / Optica 335

optica

Plasmonic enhanced silicon pyramids for internal photoemission Schottky detectors in the near-infrared regime

BORIS DESIATOV,[1] ILYA GOYKHMAN,[1] NOA MAZURSKI,[1] JOSEPH SHAPPIR,[1] JACOB B. KHURGIN,[2] AND URIEL LEVY[1,*]

[1]Department of Applied Physics, The Benin School of Engineering and Computer Science, The Center for Nanoscience and Nanotechnology, The Hebrew University of Jerusalem, Jerusalem 91904, Israel

[2]Department of Electrical and Computer Engineering, Johns Hopkins University, Baltimore, Maryland 21218, USA

*Corresponding author: ulevy@mail.huji.ac.il

Received 23 October 2014; revised 25 February 2015; accepted 26 February 2015 (Doc. ID 233599); published 1 April 2015

We demonstrate a nanoscale broadband silicon plasmonic Schottky detector with high responsivity and improved signal to noise ratio operating in the sub-bandgap regime. Responsivity is enhanced by the use of pyramidally shaped plasmonic concentrators. Owing to the large cross-section of the pyramid, light is collected from a large area which corresponds to its base, concentrated toward the nano apex of the pyramid, absorbed in the metal, and generates hot electrons. Using the internal photoemission process, these electrons cross over the Schottky barrier and are collected as a photocurrent. The combination of using silicon technology together with the high collection efficiency and nanoscale confinement makes the silicon pyramids ideal for playing a central role in the construction of improved photodetectors. Furthermore, owing to the small active area, the dark current is significantly reduced as compared with flat detectors, and thus an improved signal to noise ratio is obtained. Our measurements show high responsivities over a broad spectral regime, with a record high of about 30 mA/W at the wavelength of 1064 nm, while keeping the dark current as low as ∼100 nA. Finally, such detectors can also be constructed in the form of a pixel array, and thus can be used as focal plane detector arrays. © 2015 Optical Society of America

OCIS codes: (040.6040) Silicon; (240.6680) Surface plasmons; (040.5160) Photodetectors; (040.3060) Infrared.

http://dx.doi.org/10.1364/OPTICA.2.000335

Low-cost silicon photodetectors are the most common choice for the visible range of the spectrum. The mature CMOS technology allows the fabrication of these detectors over large areas and in large quantities. However, such detectors fail to operate at the infrared because the energy of the incident photons is smaller than the energy bandgap of silicon and is thus not sufficient for the excitation of an electron from the valence to the conduction band. As a result, most of the commercially available detectors operating in the near-infrared portion of the spectrum consist of InGaAs structures, which have a lower energy bandgap and thus can be used to detect optical signals in the near-infrared (near-IR), e.g., at the telecom band. Such detectors have been recently integrated into silicon photonics circuitry [1]. Another popular solution, which is recently implemented in silicon photonics technology, is that of Germanium detectors [2–5]. However, having an all-silicon solution for the near-IR regime still remains a challenge. Several approaches for the realization of near-IR photodetectors in silicon were demonstrated over the years including, for example, defect-mediated processes (surface and bulk states) [6–8], nonlinear processes such as two-photon absorption [9–11], and others. A different way to detect the infrared light in silicon is by using the internal photo emission (IPE) process in a Schottky barrier. When a semiconductor shares a common interface with a metal, a Schottky barrier is created. For the interface between silicon and common metals (Cu, Al, Ag, Au), the barrier's height is typically lower than the energy bandgap of silicon. Upon the absorption of photons in the metal, their energy in transferred to the conduction electrons. Assuming that the photon energy is higher than the Schottky barrier, these electrons can cross over the Schottky barrier into the semiconductor, where they are collected as a photocurrent under a reverse bias. Usually, the efficiency of this process is low due to several reasons including, e.g., momentum

2334-2536/15/040335-04$15/0$15.00 © 2015 Optical Society of America

mismatch and low volume of interaction between the photons and the electrons; yet in recent years, several configurations exploiting the use of internal photoemission have been demonstrated where the responsivity has been enhanced by the use of surface or localized plasmons [12–27]. While improved efficiency has been reported, there is still a need for better silicon photodetectors in the near-IR, with the capability to show high quantum efficiency over a broad spectral band, low dark current, and consequently high signal to noise ratio.

Motivated by this challenge, in this Letter we demonstrate an improved configuration of a silicon Schottky photodetector for the near-IR wavelength band. Our photodetector is realized using a standard fabrication technique of anisotropic chemical wet etching in which pyramidally shaped devices are created in silicon by KOH etching. Implementation of this standard microelectronic fabrication technique provides the ability to fabricate plasmonic silicon detectors with a nanometric active area without need for "nanoscale" fabrication tools such as focused ion beam (FIB) or electron beam (Ebeam) Lithography. The silicon pyramids perform as efficient and broadband light concentrators, collecting the light from a large area into a small active pixel area, thus providing high responsivity together with low dark current. Furthermore, the efficiency of the photoemission process is enhanced at the nanoscale apex of the pyramid owing to the relaxation of the electron momentum mismatch between the silicon and the metal. Finally, our structures can be constructed in the form of an array, thus performing as an efficient and low-cost focal plane array for this spectral regime. A schematic drawing of our device is depicted in Fig. 1. Light is incident from the backside of the silicon wafer and propagates toward the active pixel area, where it is concentrated by the silicon pyramid toward the apex. Owing to the large refractive index contrast between the silicon and its surroundings, most of the light is propagating below the critical angle for reflection and thus cannot escape from the pyramid.

The device was fabricated on a silicon wafer using an anisotropic etching of silicon in KOH solution. Next, the structures were planarized by an SU-8 polymer, followed by formation of Al Schottky contacts. Each fabrication step was inspected by taking optical images and scanning electron microscope (SEM) micrographs (see Supplement 1). SEM micrographs of a typical fabricated device are shown in Figs. 2(a) and 2(b). The apex of the pyramid was found to be ~50 nm. It should be noted that such a nanoscale feature was formed by the standard process of silicon oxidation in a thermal furnace, without need for nanopatterning tools such as Ebeam lithography or FIB technique (see Supplement 1 for more details).

Based on the exact dimensions of the fabricated devices as extracted from the SEM micrographs, we calculated the electric field distribution, reflection, transmission, and absorption in our device by using a three-dimensional (3D) finite-difference time-domain simulation technique. In our simulation, the pyramid structure with an aluminum cladding covering the top of its apex was illuminated by a plane wave source from the base of the pyramid at different wavelengths. A cross-section of the calculated intensity distribution at the wavelength of 1300 nm inside the pyramid near the apex is shown in Fig. 3(a). A movie showing the light propagation and absorption in the device is presented in Media 1.

At the apex of the pyramid, the electric field intensity is enhanced by a factor of ~30 compared with the electromagnetic intensity in the base of the silicon pyramid. The simulated optical absorption in the device was found to be 4% at the wavelength 1300 nm. This absorption is caused by the ohmic loses of the metal and is described by $q(\bar{r}) = \frac{\omega\varepsilon_0}{2}\mathrm{Im}(\varepsilon_{\mathrm{metal}})|\bar{E}(\bar{r})|^2$. While in most plasmonic devices Ohmic loss is considered to be harmful, here the loss plays a positive role, as it is the source of hot electron generation. Figure 3(b) shows the hot electron generation density in the device. As can be observed, most of the hot electrons are generated in the metallic part of the pyramid close to the pyramid's apex.

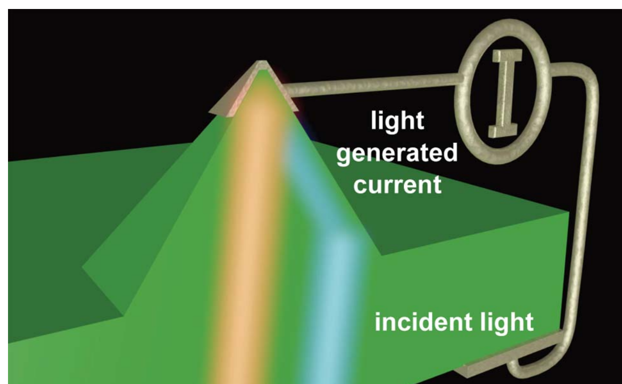

Fig. 1. Schematic representation of our device. Light is incident from the backside of the silicon wafer and propagates toward the active pixel area, where it is concentrated by the silicon pyramid toward the apex.

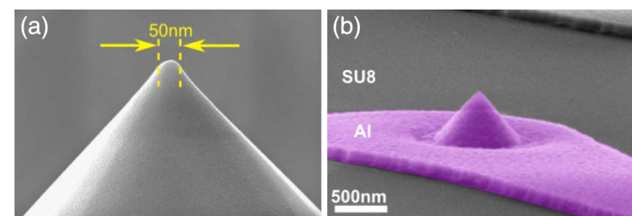

Fig. 2. SEM micrograph of a typical fabricated device. (a) Formation of the nanoapex in the silicon pyramid. (b) SEM micrograph of a final fabricated device.

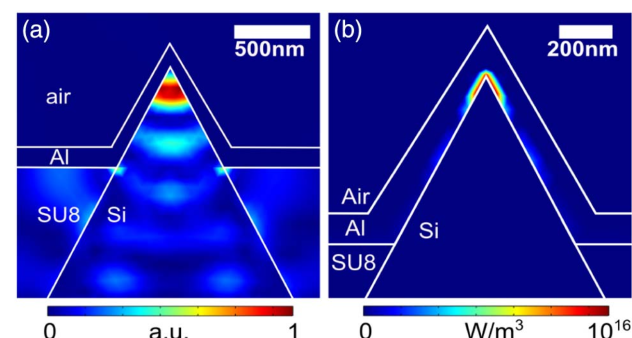

Fig. 3. (a) Calculated average electromagnetic intensity within the device at the wavelength of 1300 nm. (b) Calculated distribution of the generated hot electrons in the device. (See Media 1.)

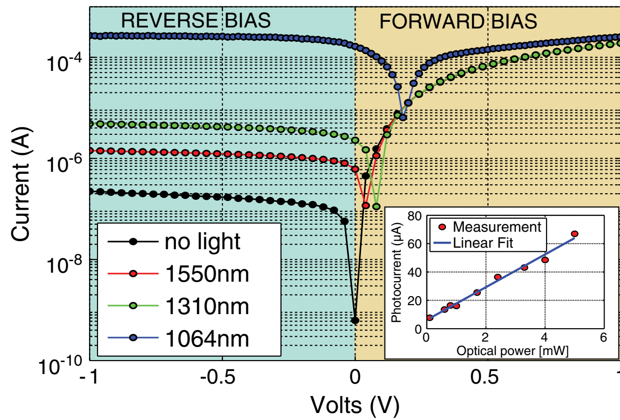

Fig. 4. I-V measurements of the pyramid Schottky device at constant optical power for three different wavelengths. For comparison, dark measurements are also presented. The inset shows the photocurrent versus optical power data and linear fit for 1550 nm wavelength.

Therefore, we may anticipate some relaxation of the momentum mismatch condition in the transfer of electrons from the metal to the semiconductor [12,22,28].

To experimentally characterize our Schottky plasmonic detector, the device was illuminated from its backside by near-infrared light derived from three different laser diode sources at three different wavelengths. The electrical detection performance of the device was characterized at room temperature (295 K) by measuring the current–voltage (I-V) characteristics of the Schottky contact under different illumination conditions. In Fig. 4, we present the measured I-V characteristic of a typical device for different wavelengths of illumination at a constant incident optical power, obtained by focusing light onto the active area of the pixel using a $F = 6$ mm lens converting the ~1 mm diameter incident beam into a small spot of about 20 μm in diameter. Without the illumination, the device shows a nonlinear asymmetric rectifying behavior with a dark current of 80 nA for reverse bias of 0.1 V. In forward bias, the diode current was limited by the serial resistance of the metal contacts, calculated to be 4 KΩ. Evidently, the photo-generated current is increasing with the energy of the photons, which is common for Schottky photodetectors and opposite from what is observed in standard photodiodes. The reason for this behavior is the rapid increase (with respect to the photon energy) in probability of the internal photoemmision process [28], which surpasses the standard $1/h\nu$ reduction in number of photons at constant optical power. To obtain the responsivity of our pyramid Schottky detector, we measured the photo-generated current under small reverse bias of 0.1 V as a function of an incident optical power. As expected, the photocurrent is linearly increasing with respect to the incident optical power, as shown in inset of Fig. 4. Additionally, the observed shift in the minimum of the current is attributed to the induced photocurrent source, which opposes the forward bias current of the Schottky diode.

The slope of the curve represents the responsivity of the device according to $I_R = I_{\text{dark}} + R \times P_{\text{in}}$, where I_{dark} is the leakage current of the Schottky diode, R is the photodetector responsivity, and P_{in} is the optical power delivered to the device. We found the responsivity of the device to be 5, 12, and 30 mA/W for incident optical wavelengths of 1550 nm, 1300 nm, and 1064 nm, respectively. The linear dynamic range (LDR), defined by $20 \log(J_{\text{ph}}/J_{\text{dark}})$ [29], was found to be 20 dB, 31 dB, and 67 dB, respectively. We fabricated a few tens of these detectors in different chips with yield of above 90%. In each batch, the responsivity was nearly the same, providing an indication for the robustness of the proposed approach. One should be aware, however, that the Schottky barrier height is strongly dependent on the surface states of the semiconductor and may be influenced strongly by varying the fabrication conditions. It should be noticed that the responsivity of our silicon detector is still lower compared to commercial InGaAs and Ge detectors [$R(1.5\ \mu\text{m}) = 0.95$ A/W $R(1.5\ \mu\text{m}) = 0.9$ A/W, respectively], yet it offers the important advantages of simplicity, compatibility with silicon, and low-cost fabrication on top of its interesting physical mechanisms.

In order to demonstrate the role of the pyramids in enhancing the performance of the device, we compare our pyramid Schottky photodetectors with a Schottky detector realized in a flat geometry using a similar fabrication process and with the same area of active plasmonic Schottky contact. Figure 5(a) shows typical I-V measurements of the two types of detectors. These measurements were performed at a wavelength of 1300 nm and at a constant optical power of 1 mW, which is focused to the 20 μm spot. Evidently, the responsivity of the pyramidally shaped detector is nearly two orders of magnitude higher compared with the flat device. This significantly higher responsivity can be partially explained simply by the collection efficiency of the pyramid, directing most of the incident optical power toward the active pixel area in the vicinity of the apex. In contrast, the flat pixel is smaller than the incident optical beam and hence most of the incident optical power is not contributing to the detection process.

The effect of light collection by the pyramid is emphasized in Figs. 5(b) and 5(d), where the numerically calculated light intensity is shown for the pyramid and the flat structure, respectively. SEM micrographs of the pyramid and the flat device are presented in Figs. 5(c) and 5(e), respectively. While the high concentration efficiency of the pyramid leads to an enhancement in the responsivity of the device, the effect of nanoscale confinement of plasmons at the apex of the tip may

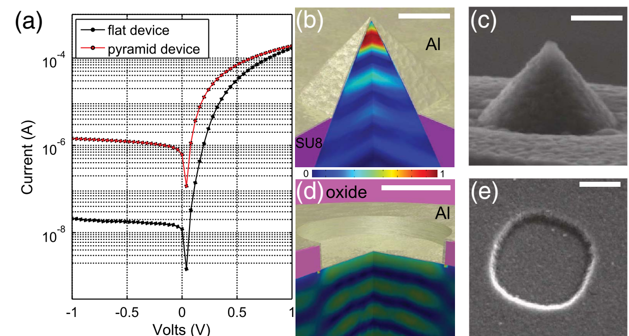

Fig. 5. (a) I-V measurements of the pyramid and the flat device. (b), (d) Calculated normalized average electromagnetic field intensities superimposed on the silicon in the 3d models. (c), (e) SEM micrographs of the fabricated devices. Scale bar is 500 nm.

also play a role via the mechanism of momentum mismatch relaxation, as has been shown before [27,29–31]. In order to address this latter issue, we fabricated several flat detectors with increasing area, and measured responsivity (see Supplement 1). Because the light absorption of the two structures is within the same order of magnitude, this result provides evidence for the significant increase in internal photoemission efficiency provided by the nanoscale confinement of electromagnetic energy next to the apex of the tip. Achieving nearly two-fold improvement in efficiency while keeping the dark current constant shows the significant advantage of our device in enhancing the signal to noise ratio by integrating pyramids for the purpose of improved collection efficiency while using a monolithic silicon process.

In summary, we have demonstrated a broadband silicon plasmonic Schottky detector with high responsivity and enhanced signal to noise ratio operating in the sub-bandgap regime. Responsivity is enhanced by the use of pyramidally shaped plasmonic concentrators. Owing to the large cross-section of the pyramid, light is collected from a large area and is concentrated toward its apex, where it absorbed in the metal and generates hot electrons. Using the internal photoemission process, these electrons cross over the Schottky barrier and are collected as a photocurrent. The combination of large collection efficiency together with nanoscale confinement makes the silicon pyramids ideal for functioning as photodetectors. Furthermore, owing to the small active area, the dark current is significantly reduced compared with a large area device, thus allowing for a significant improvement in signal to noise ratio. Our measurements show high responsivities over a very broad spectral regime, with a record result of about 30 mA/W at the wavelength of 1064 nm and dark current of about 100 nA. Finally, such detectors can also be constructed as a pixel array, and thus can be used as focal plane detector arrays.

FUNDING INFORMATION

Israel Strategic Alternative Energy Foundation; United States - Israel Binational Science Foundation (BSF).

ACKNOWLEDGMENT

B. D. and I. G. acknowledge the Eshkol fellowship from the Israeli Ministry of Science and Technology. The devices were fabricated at the Center for Nanoscience and Nanotechnology, The Hebrew University of Jerusalem.

See Supplement 1 for supporting content.

REFERENCES

1. G. Roelkens, D. Van Thourhout, R. Baets, R. Nötzel, and M. Smit, Opt. Express **14**, 8154 (2006).
2. L. Chen and M. Lipson, Opt. Express **17**, 7901 (2009).
3. S. Assefa, F. Xia, and Y. A. Vlasov, Nature **464**, 80 (2010).
4. C. T. DeRose, D. C. Trotter, W. A. Zortman, A. L. Starbuck, M. Fisher, M. R. Watts, and P. S. Davids, Opt. Express **19**, 24897 (2011).
5. L. Chen and M. Lipson, Opt. Express **17**, 7901 (2009).
6. H. Yu, D. Korn, M. Pantouvaki, J. Van Campenhout, K. Komorowska, P. Verheyen, G. Lepage, P. Absil, D. Hillerkuss, L. Alloatti, J. Leuthold, R. Baets, and W. Bogaerts, Opt. Lett. **37**, 4681 (2012).
7. B. Desiatov, I. Goykhman, J. Shappir, and U. Levy, Appl. Phys. Lett. **104**, 091105 (2014).
8. J. K. Doylend, P. E. Jessop, and A. P. Knights, Opt. Express **18**, 14671 (2010).
9. H. Chen, X. Luo, and A. W. Poon, Appl. Phys. Lett. **95**, 171111 (2009).
10. R. Hayakawa, N. Ishikura, H. C. Nguyen, and T. Baba, Appl. Phys. Lett. **102**, 031114 (2013).
11. T. K. Liang, H. K. Tsang, I. E. Day, J. Drake, A. P. Knights, and M. Asghari, Appl. Phys. Lett. **81**, 1323 (2002).
12. C. Scales, I. Breukelaar, and P. Berini, Opt. Lett. **35**, 529 (2010).
13. C. Scales and P. Berini, IEEE J. Quantum Electron. **46**, 633 (2010).
14. A. Akbari and P. Berini, Appl. Phys. Lett. **95**, 021104 (2009).
15. M. Casalino, L. Sirleto, M. Iodice, N. Saffioti, M. Gioffrè, I. Rendina, and G. Coppola, Appl. Phys. Lett. **96**, 241112 (2010).
16. Y. K. Lee, C. H. Jung, J. Park, H. Seo, G. A. Somorjai, and J. Y. Park, Nano Lett. **11**, 4251 (2011).
17. T. Aihara, K. Nakagawa, M. Fukuhara, Y. L. Yu, K. Yamaguchi, and M. Fukuda, Appl. Phys. Lett. **99**, 043111 (2011).
18. H. Chalabi, D. Schoen, and M. L. Brongersma, Nano Lett. **14**, 1374 (2014).
19. S. Zhu, H. S. Chu, G. Q. Lo, P. Bai, and D. L. Kwong, Appl. Phys. Lett. **100**, 061109 (2012).
20. I. Goykhman, B. Desiatov, J. Khurgin, J. Shappir, and U. Levy, Nano Lett. **11**, 2219 (2011).
21. I. Goykhman, B. Desiatov, J. Khurgin, J. Shappir, and U. Levy, Opt. Express **20**, 28594 (2012).
22. M. W. Knight, Y. Wang, A. S. Urban, A. Sobhani, B. Y. Zheng, P. Nordlander, and N. J. Halas, Nano Lett. **13**, 1687 (2013).
23. M. W. Knight, H. Sobhani, P. Nordlander, and N. J. Halas, Science **332**, 702 (2011).
24. A. Sobhani, M. W. Knight, Y. Wang, B. Zheng, N. S. King, L. V. Brown, Z. Fang, P. Nordlander, and N. J. Halas, Nat. Commun. **4**, 1643 (2013).
25. W. Li and J. Valentine, Nano Lett. **14**, 3510 (2014).
26. K.-T. Lin, H.-L. Chen, Y.-S. Lai, and C.-C. Yu, Nat. Commun. **5**, 3288 (2014).
27. A. Giugni, B. Torre, A. Toma, M. Francardi, M. Malerba, A. Alabastri, R. P. Zaccaria, M. I. Stockman, and E. Di Fabrizio, Nat. Nanotechnol. **8**, 845 (2013).
28. I. Goykhman, B. Desiatov, J. Shappir, J. B. Khurgin, and U. Levy, “Model for quantum efficiency of guided mode plasmonic enhanced silicon schottky detectors,” arXiv: 1401.2624 (2014).
29. X. Gong, M. Tong, Y. Xia, W. Cai, J. S. Moon, Y. Cao, G. Yu, C.-L. Shieh, B. Nilsson, and A. J. Heeger, Science **325**, 1665 (2009).
30. A. O. Govorov, H. Zhang, and Y. K. Gun’ko, J. Phys. Chem. C **117**, 16616 (2013).
31. H. Zhang and A. O. Govorov, J. Phys. Chem. C **118**, 7606 (2014).